ELSEVIER

Design and fabrication of electro-optic waveguides with self-assembled superlattice films

De-Gui Sun[a],*, Zhifu Liu[b], Jing Ma[b], Seng-Tiong Ho[b]

[a]*State Key Laboratory of Applied Optics, Changchun Institute of Optics, Fine Mechanics and Physics, Chinese Academy of Sciences, 16 East Nanhu Street, Changchun, JL 130031, China*
[b]*Department of Electrical and Computer Engineering, Northwestern University, Evanston, IL 60208, USA*

Abstract

This paper presents a strategy for fabricating low loss waveguide devices based on high electro-optic (EO) coefficient self-assembled superlattice (SAS) films, a new sort of polymeric films grown on SiO_2 film and coated with other polymeric films to form multi-layer EO waveguides structure without electric field poling. Firstly, the optical propagation loss induced by the absorption of electrodes is simulated and optimized to obtain both the low optical loss and the low drive voltage. Then this paper gives the scanned electron microscopic (SEM) images of the fabricated devices, the simulated and experimental images of the single guided mode, and the measured optical propagation loss of the EO waveguide devices of 1.0 dB/cm. Finally, the very great agreement between the simulated and measured results of propagation loss of devices is observed.
© 2005 Elsevier Ltd. All rights reserved.

Keywords: Electro-optic polymer; Self-assembled superlattice; Low loss waveguide

1. Introduction

Electro-optic (EO) devices including high-speed modulators, switches, etc. are popular components in modern optical communications and optical signal processing systems. For EO modulators, their main performance is evaluated according to the modulation bandwidth, the drive voltage, device size, manufacturability and so forth. Organic materials containing molecular units with large second-order nonlinear susceptibilities are attractive for high-speed lightwave modulation [1–3]. In particular, polymer-based EO modulators have been studied for a long time and had impressive accomplishments in research such as the demonstration for high-speed modulation from 40 to 110 GHz [3–5].

Polymer-based devices are easy to be fabricated with micro-strip electrode geometries that give a large optical/electrical overlap in modulating devices [4,5]. However, polymers, especially the poled polymers, still present critical challenges before polymer-based EO devices are commercialized. These challenges include an undesirable intrinsic optical absorption, poling-induced damage to the physical properties, and a lack of substantiated proof of long-term stability [5]. Self-assembled superlattice (SAS) classes of materials [6] have potentially larger nonlinear EO responses than conventional glassy polymers and do not require electric field poling. Thus they are attractive for high-speed, low drive voltage EO modulating devices and have temporal stability of the EO properties [7]. The SAS-based EO devices require different considerations in device optimization from those of poled-polymer EO device structures. This paper presents an optimized structure to achieve low drive voltages in SAS-based waveguides for EO devices.

2. Analysis for optical propagation loss

Recently, the reliable SAS thickness that can be achieved was increased to 0.2–0.5 μm. However, this thickness is insufficient for the SAS component to be the exclusive core layer of an EO waveguide. Thus, the polymer benzocyclobutene (BCB), which has a refractive index close to that of

*Corresponding author.
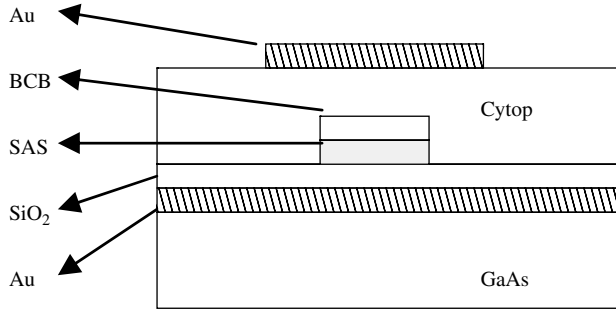E-mail address:* deguisun_b@yahoo.com (D.-G. Sun).

Fig. 1. Schematic of a SAS-based EO waveguide device.

the SAS film, is introduced as co-guiding layer together with the SAS film in the device structure. Fig. 1 shows a schematic of an EO waveguide structure using the SAS material as the EO-active component. This EO waveguide structure is basically composed of a multiple-layer waveguides system and electrodes system. Here the upper cladding layer is the polymer CYTOP, the co-guiding layer contains BCB film and SAS film, the lower cladding layer is SiO$_2$, and the electrode is gold [8,9]. An EO waveguide device is firstly required to have a relatively low half-wave drive voltage defined by, [10]

$$V_\pi = \frac{\lambda D}{n_{\text{sas}}^3 r \Gamma L},\tag{1}$$

where λ is the wavelength of light wave in free space, r the EO coefficient of the SAS film, n the optical refractive index of the SAS film, D the distance between the upper and lower electrodes, L the interaction length, and Γ the overlap integral of optical and electrical fields in the EO waveguide and can be simply calculated by $\Gamma \approx t/(t+d)$ with assuming the electrode is enough wide, where t and d are the thickness of SAS film and the thickness of BCB film, respectively, in waveguide. Note that from Eq. (1), there should be a larger L value and a lower D value to obtain a lower drive voltage V_π value, but a larger L and a lower D can result in a higher optical propagation loss, so it is very necessary to optimize the system.

3. Theoretical study

In order to achieve a low half-wave drive voltage, it is desirable to minimize the distance between the top and the bottom Au electrodes by minimizing the thickness of the upper and lower cladding layers. However, when the cladding thickness is small, the optical modes will begin to have substantial optical loss, especially for the TM modes, due to optical absorption by the Au electrodes. Another impact of changing the electrode distance is the change in the propagation impedance of the parallel plate transmission lines formed by the top and bottom electrodes referred to as micro-strip electrodes. Namely, a low optical loss design is crucial for a SAS-based EO device when the

thickness of SAS film is insufficient as an exclusive core of the EO waveguide. In order to achieve this goal, a fast and efficient theoretical method has been demonstrated [11]. This method offers a numerical analysis of vertical wave propagation in waveguides with arbitrary refractive properties for calculating the modal properties in a waveguide with an arbitrary refractive index distribution. If the waveguide system contains N layers labeled by $i(i = 1, 2, \ldots, N)$, and the layer 0 is the substrate, the angle for the lowest-order guided mode corresponds to the lowest angle that results in a local maximum for the field excitation in the waveguide, which is referred to as the fundamental mode, and hence a local maximum transmittance is formed in the waveguide. This angle can be used to propagate through the medium and calculate the field at each layer in the waveguide as a function of space. Then, the relations among the transmittance τ, the reflectance r and the optical propagation loss A induced by Au absorption of the system can be defined by [11,12]

$$\tau = \frac{4\eta_0 \eta_s}{(B\eta_N + C)\cdot(B\eta_N + C)^*},\tag{2a}$$

$$r = \frac{(B\eta_N - C)\times(B\eta_N - C)^*}{(B\eta_N + C)\times(B\eta_N + C)^*},\tag{2b}$$

$$\tau^2 + r^2 + A = 1,\tag{2c}$$

where

$$\begin{pmatrix} B \\ C \end{pmatrix} = \prod_{i=1}^{N} \begin{pmatrix} \cos\delta_i & j/\eta_i \sin\delta_i \\ j\eta_i \sin\delta_i & \cos\delta_i \end{pmatrix} \times \begin{pmatrix} 1 \\ \eta_s \end{pmatrix},\tag{3}$$

$$\tau = (2\pi/\lambda)L_i N_i \cos\delta_i,\tag{4}$$

$$\eta_i = \begin{cases} N_i \cos\theta_i & (\text{for S wave}), \\ N_i/\cos\theta & (\text{for P wave}), \end{cases}\tag{5}$$

$$N_i = n_i - k_i,\tag{6}$$

where η_i is the optical conductance of the ith layer film and, in a similar manner, η_o and η_s are the optical conductance values of the air and the substrate, respectively. Here N_i is the complex index of the ith layer film, and n_i, k_i, and θ_i are the effective index, extinction coefficient, and the refractive angle of the ith layer film.

4. Optimization for optical loss

In order to obtain the desirable operation for the EO waveguide systems described by Eq. (1), we simulated optical propagation loss of single-mode waveguides, where only the TM modes were considered. In the simulation, the wavelength in free space is $\lambda = 1550$ nm. At this wavelength, we take the refractive index of the core layer material BCB as $n_{\text{core}} = 1.56$, which is very close to the measured value of refractive index of the SAS film, the refractive index of the lower cladding layer SiO$_2$ $n_{\text{lc}} = 1.45$, and the refractive index of the upper commercially

available cladding layer CYTOP $n_{uc} = 1.34$ [8,9]. In addition, the Au, as the electrode material, has a complex index expressed as $n_s = 0.38 + 10.4j$. It is obvious that for BCB, SiO$_2$ and CYTOP, the extinction coefficients: k_{core}, k_{lc} and k_{uc} are all taken as 0. We know that the thickness of the core layer, and of the upper and the lower cladding layers directly impacts the Au electrode absorption loss, and both the upper and the lower Au electrodes have the same level of absorption losses.

With Eqs. (2)–(6) and the above parameters, we find that when the thickness of the upper cladding layer CYTOP is larger than 1.0 μm, the absorption loss induced by the upper Au electrode can be ignorable, so we omitted the upper Au electrode by using a sufficiently thick CYTOP upper cladding layer. Accordingly, we mainly study the influences of the waveguide core layer BCB thickness and the thickness of the lower cladding layer, SiO$_2$. First, the relation between the Au absorption loss and BCB thickness was obtained as shown in Fig. 2(a). Note from Fig. 2(a) that the thickness of either the lower cladding layer SiO$_2$ or the waveguide core layer BCB impacts the optical absorption loss of the bottom Au electrode. At both the 2.0 and 2.5 μm thickness of SiO$_2$, the optical absorption loss of the Au film quickly decreases with the thickness of the waveguide core layer BCB in the range from 1.1 to 1.4 μm, but it slowly decreases when the BCB thickness is larger than 1.4 μm. Our simulation shows that the thickness range of the waveguide core BCB layer for single-mode operations is 1.0–1.4 μm. In the same manner, the relation between the Au absorption loss and SiO$_2$ thickness was obtained as shown in Fig. 2(b). Note from Fig. 2(b) that when the SiO$_2$ thickness is larger than 2.6 μm and the BCB thickness is 1.4 μm, the Au absorption is less than 1.0 dB/cm. For the EO waveguide device, the Au absorption loss of less than 1.0 dB/cm is sufficient for achieving a low half-wave drive voltage V_π and very helpful for increasing the device length in fabrication of SAS based EO waveguide devices. In above simulation, the top Au electrode is removed away and the optical signal is input from top, so the absorption loss results are only from the bottom electrode. The absorption loss induced by the top electrode can be simulated with an inverse construction as that in the case of bottom electrode, and the sum of these two cases is total absorption loss of the system. Namely, in the simulation for the absorption loss from the top electrode, both the bottom electrode and the substrate are removed away, and the optical signal is input from bottom.

5. Fabrication and experiments

In accordance with the simulated results above, the characteristics of the SAS film, polymers BCB and CYTOP, a successful program for fabricating the SAS-based EO waveguide devices is designed as shown in Fig. 3. In this program, the selection for the substrate of GaAs is based on the growing process of SAS films. With this
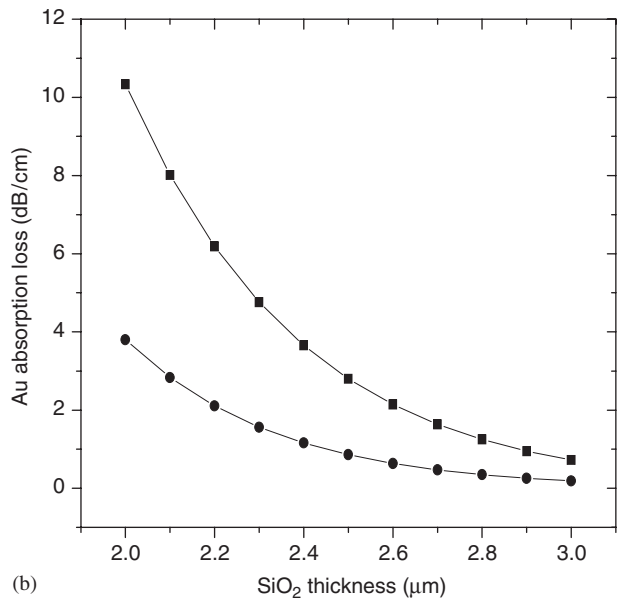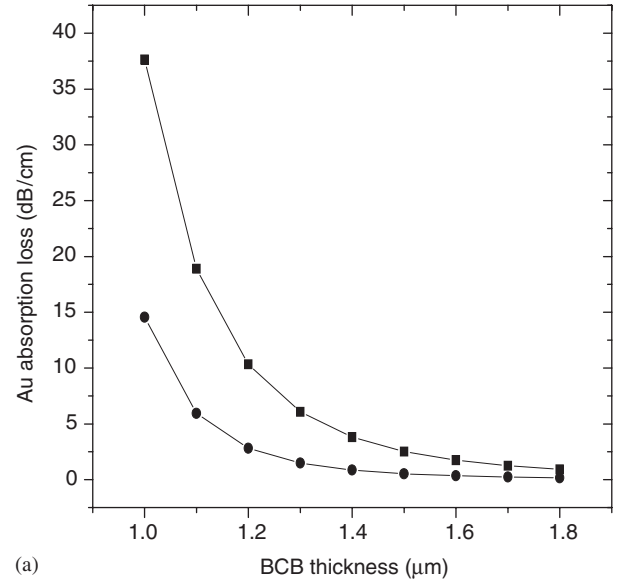
(a)

(b)

Fig. 2. (a) Au absorption vs. BCB thickness for different SiO$_2$ cladding thickness: solid squares are for 2.0 μm SiO$_2$ and solid circles are for 2.5 μm SiO$_2$, and (b) Au absorption vs. SiO$_2$ thickness for different BCB thickness: solid squares are for 1.2 μm BCB and solid circles are for 1.4 μm BCB.
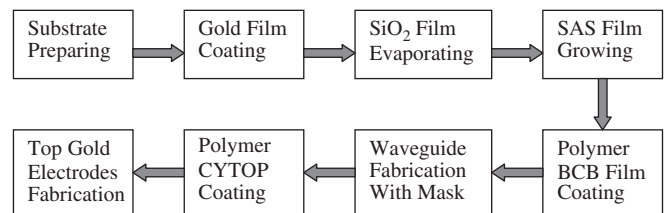
Fig. 3. A typical program for the SAS-based EO waveguide device.

fabricating program, we fabricated some device samples including both straight waveguide and Y-junction wave-guide structures. These samples have two different thickness

values of SiO_2: 2.0 and 2.65 μm with respect to the two cases of SiO_2 film, and two different thickness values of BCB layer: 1.2 and 1.4 μm. The two structures of waveguide samples: the straight waveguide and the Y-junction waveguide are the two popular cases in EO
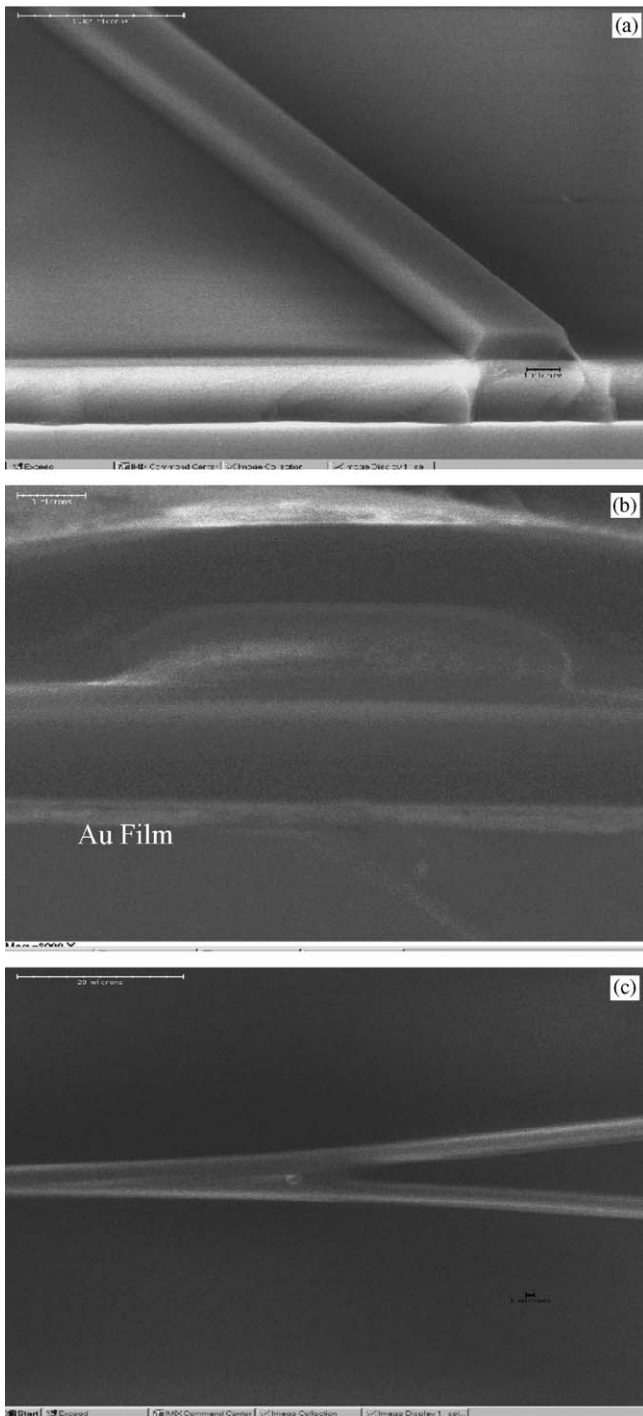

Fig. 4. (a) SEM perspective image of BCB and SAS-based waveguide channel before upper cladding layer CYTOP deposition for EO modulator, (b) SEM cross-sectional image of SAS-based EO modulators, and (c) SEM top view image of SAS-based Y-junction waveguide structure.

waveguide devices. The SEM perspective image of the straight waveguide (before the upper cladding CYTOP was coated) is shown in Fig. 4(a), the cross-sectional image of this structure (after the upper cladding was coated) is shown in Fig. 4(b), and an SEM top view image of Y-junction waveguide is shown in Fig. 4(c). The excellent fabricating quality of the multi-layer waveguide structure could be observed with ease from these SEM images. These samples are used for analyzing the waveguide quality and the propagation loss measurements. Qualification of these two waveguide structures implies that the fabrication of the waveguide system is acceptable. With these samples, the measured results of optical propagation losses are obtained and summarized in Table I. In the experiments, the coupling loss at the two ends of the test device was reasonably estimated. Note that the measured results agree well with the simulated values, which strongly supports the efficiency of the design method and the fabricating program in this work.

Further with R-Soft simulation tool and the above parameters, we obtain the simulated result of electric field distribution of the single-mode wavegude as shown in Fig. 5(a), and with the fabricated sample as shown in Fig. 4(a), we obtain the experimental result of the guided mode output as shown in Fig. 5(b). The great agreement between the simulated result shown in Fig. 5(a) and the experimental result shown in Fig. 5(b) further strongly supports the efficiency of design method studied in this work.

6. Conclusions

In this SAS film-based EO multi-layer waveguide structure, polymer BCB is used as co-guiding layer, and the SiO_2 film and the other polymer CYTOP film are used as lower and upper cladding layers, respectively, and the Au strip electrodes are employed. An efficient theoretical method for calculating optical propagation loss induced by Au electrode is presented and the excellent agreement between the experimental and the simulated results of optical propagation loss have been achieved. Further, the simulated guided image and the experimental image of single mode are given, and the agreement between the simulated and the experimental images of the optimal samples is observed. In this work, the art-state fabricating program for this kind of devices is very helpful for research and development of the new kind of SAS-based EO

Table 1
Measured results of optical loss induced by the bottom electrode ($\lambda = 1550$ nm)

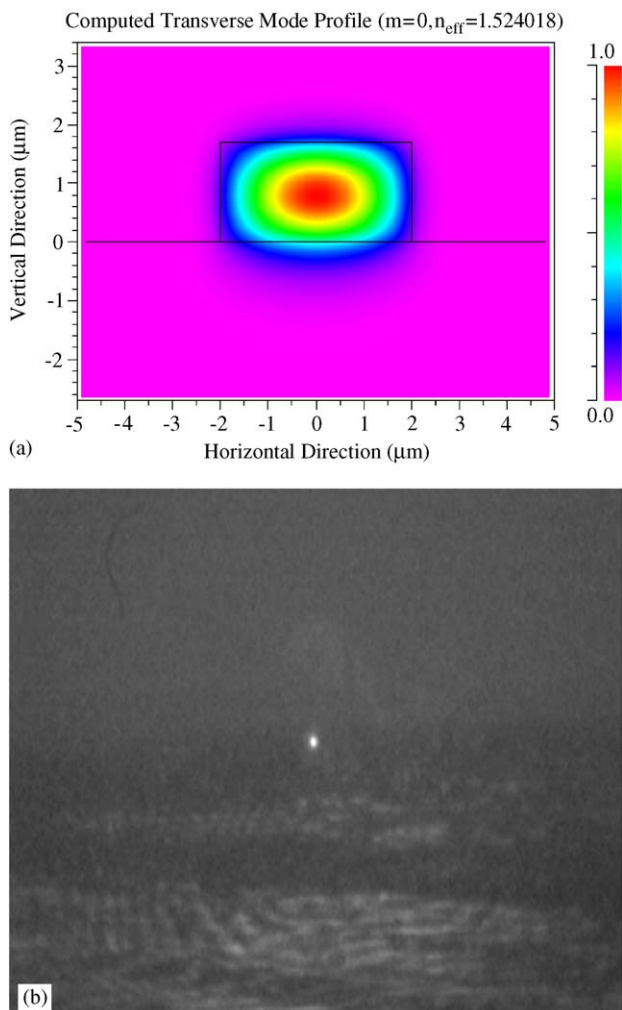| SiO_2 thickness	2.00 (μm)	2.65 (μm)	2.65 (μm)
Core BCB thickness (μm)	1.0–1.1	1.1–1.2	1.3–1.4
Metal loss (dB/cm)	~20	~7.0	<1.0

Fig. 5. Typical optical single-mode profiles within the waveguide: (a) the simulated result and (b) the experimental result.

waveguide devices and it can become easier as the thickness of SAS films is sufficiently thick to be an exclusive layer of the EO waveguide devices.

References

[1] Shuto Y, Tomaru S, Hikita M, Amano M. Optical intensity modulators using diazo-dye-substituted polymer channel waveguides. IEEE J Quantum Electron 1995;31(8):1451–60.

[2] Chen D, Fetterman HR, Chen A, Steier WH, Dalton LR, Wang W, et al. Demonstration of 110 GHz electro-optic polymer modulators. Appl Phys Lett 1997;70(25):3335–7.

[3] Eldada L, Shacklette W. Advances in polymer integrated optics. IEEE J Sel Top Quantum Electron 2000;6(1):54–68.

[4] Oh MC, Zhang H, Zhang C, Erlig H, Chang Y, Tsap B, et al. Recent advances in electro-optic polymer modulators incorporating highly nonlinear chromophore. IEEE J Sel Top Quantum Electron 2001; 7(2):826–35.

[5] Gill DM, Chowdhury A. Electro-optic polymer-based modulator design and performance for 40 Gb/s system applications. J Lightwave Technol 2002;20(12):2145–53.

[6] Zhu P, van der Boom ME, Milko E, Kang H, Evmenenko G, Dutta P, et al. Realization of expeditious layer-by-layer siloxane-based self-assemly as an efficient route to structurally regular acentric super-lattices with large electro-Ooptic responses. Chem Mater 2002;14: 4949–82.

[7] Lin WB, Lin WP, Wong GK, Marks TJ. Supramolecular approaches to second-order nonlinear optical materials. Self-assembly and microstructural characterization of intrinsically acentric [(Aminophe-nyl)azo]pyridinium superlattices. J Am Chem Soc 1996;118:8034–42.

[8] BCB 3022-25, from Dow Chemical Co., Midland, MI.

[9] Asahi Glass Co., C/O Bellex International Corp., Wilmington, DE.

[10] Shi Y, Zhang C, Zhang H, bechted JH, Dalton LR, Ronbinson BH, et al. Low (sub-1-volt) halfwave voltage polymeric electro-optic modulators achieved by controlling chromophore shape. Science 2000;288:119–22.

[11] Rafizadeh D, Ho ST. Numerical analysis of vectorial wave propagation in waveguides with arbitrary refractive index profiles. Opt Commun 1997;141:17–20.

[12] Sun DG, Wang NX, Weng ZH, Yang SM, Z Feng J. Calculation and design for bistable optical devices of nonlinear interference filters. Opt Eng 1993;32:63–6.